

# Effects of stoichiometry, purity, etching and distilling on resistance of $\text{MgB}_2$ pellets and wire segments

R. A. Ribeiro, S. L. Bud'ko, C. Petrovic, P. C. Canfield

*Ames Laboratory and Department of Physics and Astronomy  
Iowa State University, Ames, IA 50011 USA*

---

## Abstract

We present a study of the effects of non-stoichiometry, boron purity, wire diameter and post-synthesis treatment (etching and Mg distilling) on the temperature dependent resistance and resistivity of sintered  $\text{MgB}_2$  pellets and wire segments. Whereas the residual resistivity ratio ( $RRR$ ) varies between  $RRR \approx 4$  to  $RRR \geq 20$  for different boron purity, it is only moderately affected by non-stoichiometry (from 20% Mg deficiency to 20% Mg excess) and is apparently independent of wire diameter and presence of Mg metal traces on the wire surface. The obtained set of data indicates that  $RRR$  values in excess of 20 and residual resistivities as low as  $\rho_0 \approx 0.4 \mu\Omega\text{cm}$  are intrinsic material properties of high purity  $\text{MgB}_2$ .

*Key words:*  $\text{MgB}_2$ , stoichiometry, transport properties

*PACS:* 74.70.Ad, 74.25.Fy

---

## 1 Introduction

Within weeks of the announcement of the discovery of superconductivity in  $\text{MgB}_2$  by Akamitsu and co-workers [1,2], it was established that high purity, very low residual resistivity samples of  $\text{MgB}_2$  could be synthesized by exposing boron powder or filaments to Mg vapor at temperatures at or near  $950^\circ\text{C}$  for as little as two hours [3–5]. Samples with residual resistivity ratio [ $RRR = R(300\text{K})/R(42\text{K})$ ] values in excess of 20 and residual resistivities as low as  $0.4 \mu\Omega\text{cm}$  were synthesized by this method. Such a low resistivity in an intermetallic compound with a superconducting critical temperature,  $T_c$ , near  $40\text{K}$  was of profound physical, as well as engineering, interest. The implications of this high  $RRR$  and low  $\rho_0$  ranged from large magneto-resistances (in accordance with Kohler's rule) to questions of how a material with such an

apparently large electron-phonon coupling could have such a small resistivity. On the applied side, a normal state resistivity of  $0.4 \mu\Omega cm$  for temperatures just above  $T_c$  means that  $MgB_2$  wires would be able to handle a quench with much greater ease than, for example,  $Nb_3Sn$  wires which have a  $\rho_0$  that is over an order of magnitude larger for  $T \sim 20K$  [5].

Unfortunately other techniques of synthesizing  $MgB_2$  have not yet been able to achieve such high  $RRR$  or low  $\rho_0$  values [6–10]. In some cases the authors of these papers have concluded that the resistivity of their samples must be the intrinsic resistivity and that higher  $RRR$  values or lower residual resistivity values must somehow be extrinsic. In order to address these concerns and in order to shed some light on how low resistivity samples can be grown we have studied the effects of boron purity and magnesium stoichiometry on sintered pellet samples. In addition we have studied the effects of filament diameter and post synthesis etching and distilling on  $MgB_2$  wire segments. Based on these measurements we conclude that the purity of the boron used to make the  $MgB_2$  is a dominant factor in determining the ultimate, low temperature, normal state resistivity of the sample, and that  $RRR$  values as high as 20 and residual resistivities as low as  $0.4 \mu\Omega cm$  are intrinsic materials properties of high purity  $MgB_2$ .

## 2 Sample synthesis

Samples of  $MgB_2$  for this study were made in the form of sintered pellets as well as wire segments. The sintered pellets were made by sealing stoichiometric amounts of Mg and B into Ta tubes and placing these tubes (sealed in quartz) into furnaces heated to  $950^\circ C$  for 3 hours and then quenched to room temperature [3]. For the initial studies of boron purity stoichiometric  $MgB_2$  was synthesized and the quality of the boron was varied. For the studies of magnesium stoichiometry nominal stoichiometries that ranged from  $Mg_{0.8}^{11}B_2$  to  $Mg_{1.2}^{11}B_2$  were used and samples were synthesized with isotopically 99.95% enriched  $^{11}B$ . For all synthesizes lump Mg of 99.9% purity was used.

Wire segments of  $MgB_2$  were made by sealing boron filaments purchased from Textron [11] or Goodfellow [12] into a Ta tube with excess Mg, using a ratio of approximately  $Mg_3B$ . After reacting the filaments for 68 hours at  $950^\circ C$  the Ta tubes were quenched to room temperature and the wire segments were removed from the Ta reaction vessel. Given that there can be some excess Mg on the surface of the wire segments, some of the wire segments were etched in a solution of 5% HCl and ethyl alcohol for times up to 5 minutes. This treatment removes the surface Mg and leads to the surface of the wire segments having the same appearance as the surface of the stoichiometric sintered pellets: a slightly golden / grey color. Another method was used to remove any potential

surface Mg from the  $\text{MgB}_2$  wire segments: high temperature distillation of the Mg. In order to achieve this a wire sample was placed into a quartz tube that was continuously pumped by a turbomolecular pump to a pressure less than  $10^{-5}\text{ Torr}$ . The evacuated tube was then heated to  $600^\circ\text{C}$  for 12 hours. This temperature and time were chosen in part because attempts at higher temperature distillation lead to a decomposition of the  $\text{MgB}_2$  in the wire itself.

A.C. electrical resistance measurements were made using Quantum Design MPMS and PPMS units. Platinum wires for standard four-probe configuration with connected to the sample with Epotek H20E silver epoxy. LR 400 and LR 700 A.C. resistance bridges were used to measure the resistivity when the MPMS units were used to provide the temperature environment. Powder X-ray diffraction measurements were made using a  $\text{Cu } K_\alpha$  radiation in a Scintag diffractometer and a Si standard was used for all runs. The Si lines have been removed from the X-ray diffraction data, leading to apparent gaps in the powder X-ray spectra.

### 3 Effects of Boron Purity

Table 1: Boron form and purity (As provided by the seller).

Purity	Form	Source	Main Impurities
90%	Amorphous (325 mesh)	Alfa Aesar	Mg 5%
95%	Amorphous ( $< 5$ mesh)	Alfa Aesar	Mg 1%
98%	Crystalline (325 mesh)	Alfa Aesar	C 0.55%
99.95%	Isotopically pure $^{11}\text{B}$ Crystalline (325 mesh)	Eagle-Picher	Si 0.04%
99.99%	Amorphous (325 mesh)	Alfa Aesar	Metallic Impurities 0.005%

Table 1 presents the source and purity information available for each of the starting boron powders used. Figure 1 presents powder X-ray diffraction spectra for three samples with varying nominal boron purities: 90% purity, 99.99% purity, and the 99.95% purity, isotopically pure  $^{11}\text{B}$ . By comparing the two upper panels to the bottom panel it can be seen that the strongest  $\text{MgB}_2$  lines are present in all three samples. The upper panel, the data taken on the

sample made from boron with only a nominal 90% purity, also has a weak Mg and MgO powder lines present. This is not inconsistent with the fact that the primary impurity in the 90% boron is associated with Mg.

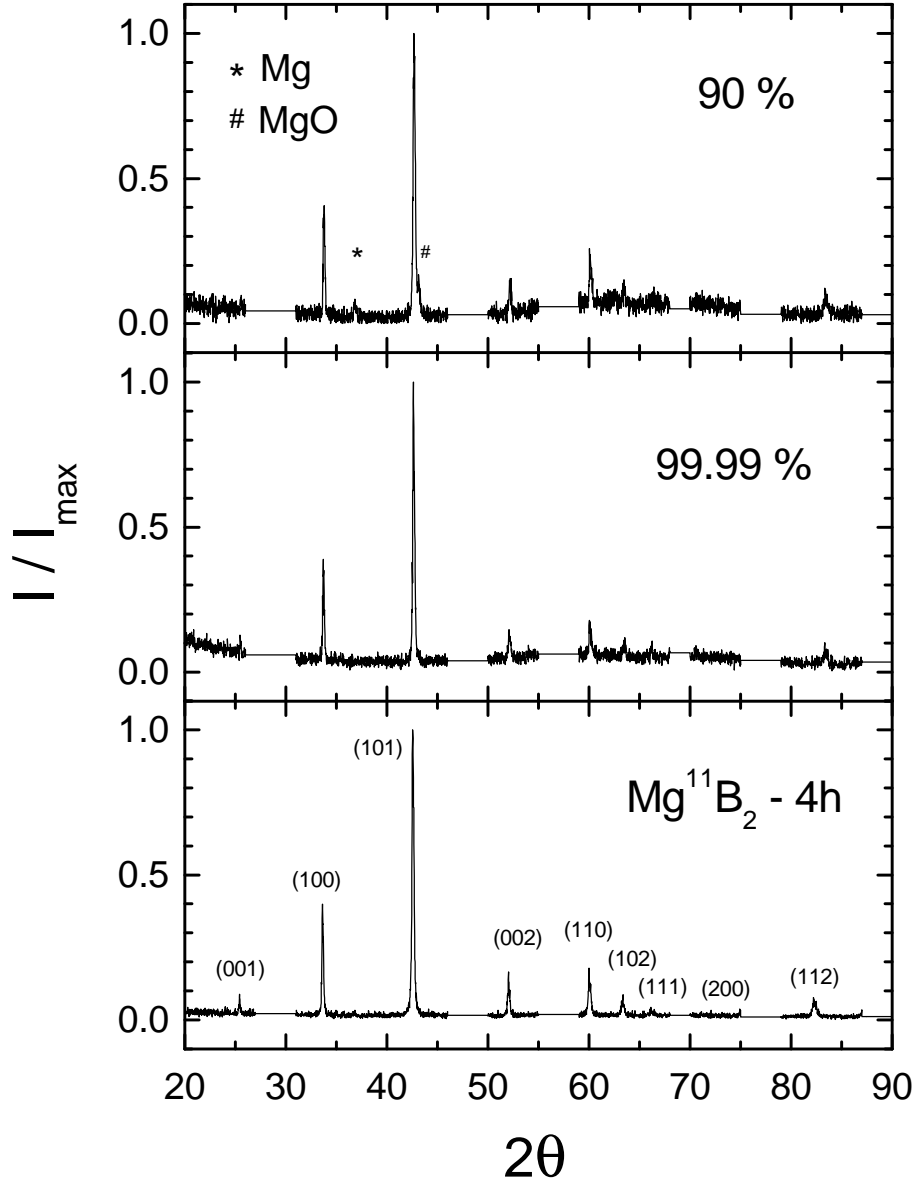


Fig. 1. Powder x-ray ( $\text{Cu } K_\alpha$  radiation) diffraction spectra of  $\text{MgB}_2$  (with  $h, k, l$ ) for 3 different qualities (a) pure natural boron 90% ; (b) pure natural boron 99.99% and (c) isotopic  $^{11}\text{B}$  99.95%. Samples (a) and (b) were synthesized for  $3h/950^\circ\text{C}$ , and sample (c) for  $4h/950^\circ\text{C}$  from [13]. The data gaps are due to the removal of the Si peaks. The symbol  $*$  indicates a Mg peak and  $\#$  indicates a MgO peak.

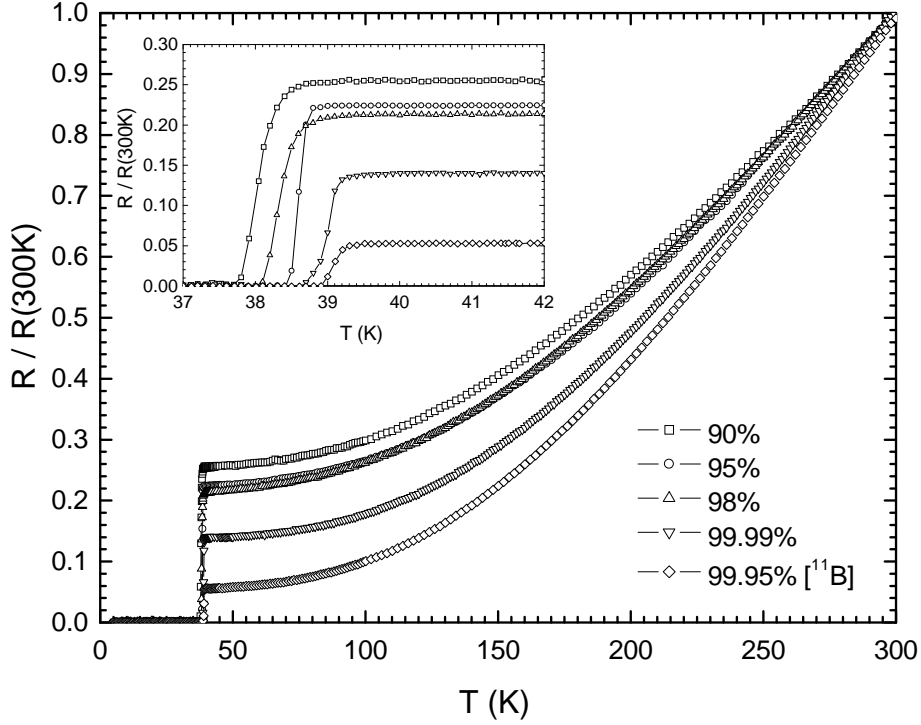


Fig. 2. Variation of the zero-field resistivity in the  $5K$  to  $300K$  range for  $MgB_2$  pellets with different boron purities. Inset shows a closeup at  $T_c$ .

Figure 2 displays the normalized resistance,  $R(T)/R(300K)$ , of  $MgB_2$  pellets that were made using five different types of boron powder. Each curve is the average of three resistivity curves taken on different pieces broken off of each pellet. Figure 2 demonstrates that  $RRR$  values can range from as low as 4 to as high as 20 depending upon what source of boron is used. Among the natural boron samples examined there is a steady increase in  $RRR$  as the purity of the source boron is improved. The  $MgB_2$  synthesized from the isotopically pure boron appears to have the best  $RRR$ , although it's nominal purity is somewhat less than that of the 99.99% pure natural boron, but those skilled in the art will realize that claims of purity from different companies can vary dramatically. In addition, it is very likely that the isotopically pure boron was prepared in a somewhat different manner from the other boron powders used (very likely using a boron fluoride or boric acid or any of its complexes as an intermediate phase in order to achieve isotopic separation). The primary point that figure 2 establishes is that the purity of the boron used can make a profound difference on the normal state transport properties.

In Fig. 3 the same resistance data is plotted, but instead of simply normalizing the data at room temperature the data is normalized to the temperature derivative at room temperature. This is done to see if the resistance curves

differ only by a temperature independent residual resistivity term: i.e. this normalization is based upon the assumption that the slope of the temperature dependent resistivity at room temperature should be dominated by phonon scattering and therefore be the same for each of these samples. As can be seen this seems to be the case, at least to the first order. By using higher purity boron we are able to diminish the additive, residual resistance by a factor of approximately five.

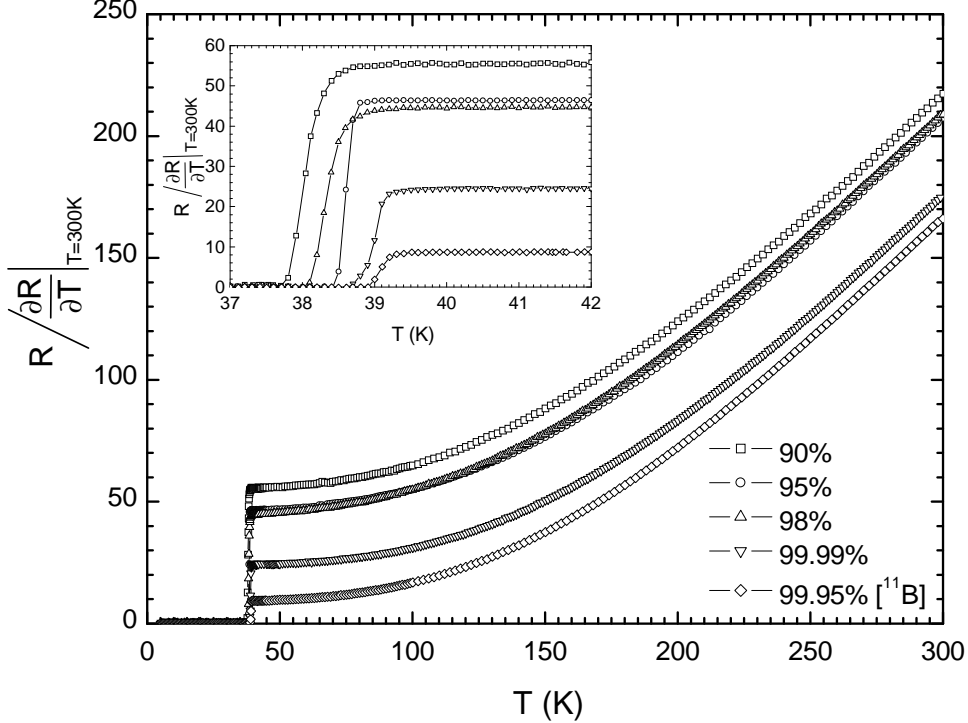


Fig. 3. Resistivity curves normalized by temperature derivative at room temperature, for different boron purities.

The insets to figs. 2 and 3 also indicate that there is a monotonic improvement in  $T_c$  as the boron purity (or  $RRR$  value) is increased.  $T_c$  values vary from just below  $38K$  to just above  $39K$  depending upon which boron is used.

Based upon these results we choose the isotopically pure  $^{11}B$  for the further study of the effects of Mg stoichiometry on  $MgB_2$  pellet samples. But before we proceed to the next section it is worth noting that one of the difficulties associated with the samples made by other research groups may well be due to the use of boron with less than the highest purity. In addition, to our knowledge very few other groups have been using the Eagle-Picher isotopically pure boron in the samples for electrical transport measurements.

#### 4 Effects of Magnesium Stoichiometry

In order to study the effect of magnesium stoichiometry on the transport properties of  $\text{Mg}^{11}\text{B}_2$  a series of  $\text{Mg}_x^{11}\text{B}_2$  ( $0.8 \leq x \leq 1.2$ ) samples were synthesized. Figure 4 presents powder X-ray diffraction patterns for the extreme members

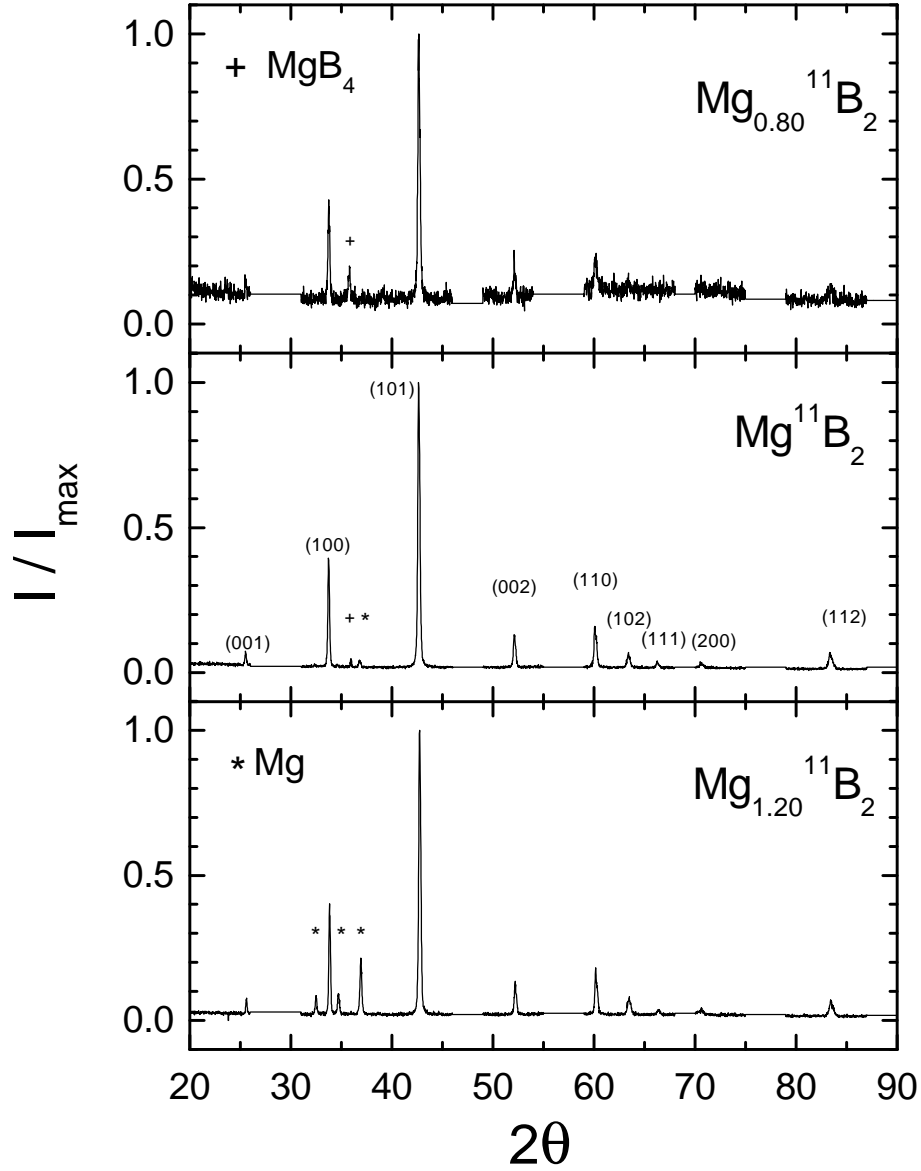


Fig. 4. X-ray spectra for three different nominal compositions of  $\text{Mg}_x^{11}\text{B}_2$  for  $x = 0.8, 1.0, 1.2$ . The symbols  $\star$  indicates Mg peaks and  $+$  indicates  $\text{MgB}_4$  peaks.

of the series (top and bottom panels) as well as for the stoichiometric  $\text{Mg}^{11}\text{B}_2$  (middle panel). In all cases the lines associated with the  $\text{Mg}^{11}\text{B}_2$  phase are present. For the  $\text{Mg}_{0.8}^{11}\text{B}_2$  sample there is a weak line seen at  $2\theta = 35.8^\circ$  that is associated with  $\text{MgB}_4$  (marked with a +). This is consistent with the fact that there was insufficient Mg present to form single phase  $\text{Mg}^{11}\text{B}_2$ . For the  $\text{Mg}_{1.2}^{11}\text{B}_2$  sample there are very strong diffraction lines associated with Mg (marked with \*). This too is consistent with the stoichiometry of the sample:  $\text{Mg}^{11}\text{B}_2$  is the most Mg-rich member of the binary phase diagram, therefore any excess Mg will show up as unreacted Mg. The X-ray diffraction pattern for the stoichiometric  $\text{Mg}^{11}\text{B}_2$  shows much smaller peaks associated with a small amount of both  $\text{MgB}_4$  and Mg phases. This pattern is different from the one shown in Fig. 2 in that this sample was reacted for three hours whereas the sample used in Fig. 2 was reacted for four hours. Given that all of the samples used for the Mg-stoichiometry study were reacted for 3 hours it is appropriate to show this powder diffraction set along with the other members of the series. It should be noted that there is continuous change in the nature of the second phases in the samples. For Mg deficient samples there is only  $\text{MgB}_4$  as a second phase. For the stoichiometric  $\text{Mg}^{11}\text{B}_2$  samples there are either no second phases or very small amounts of both  $\text{MgB}_4$  and Mg (depending upon reaction times), and for the excess Mg samples there is no  $\text{MgB}_4$ , but clear evidence of excess Mg.

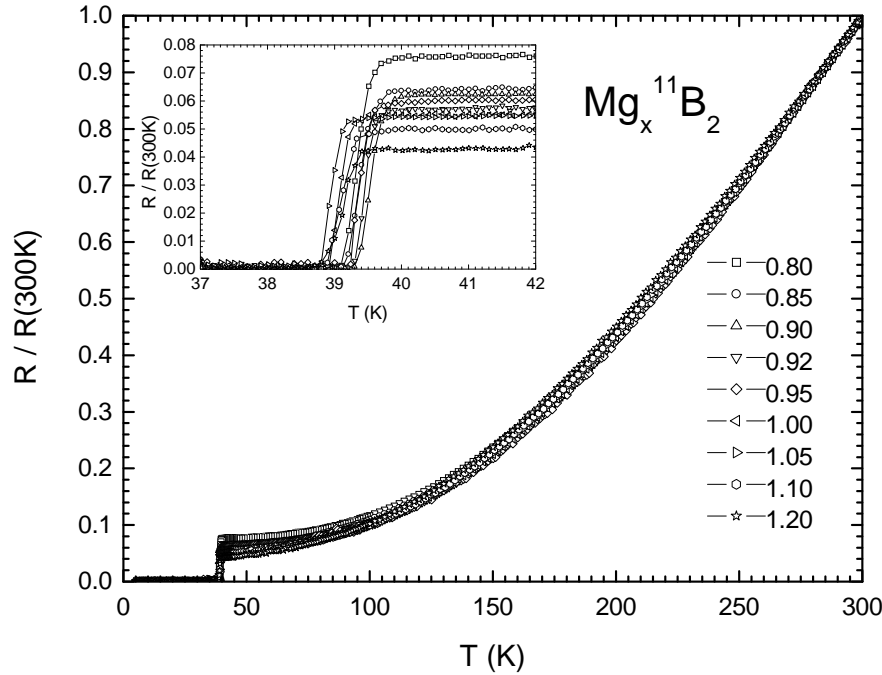


Fig. 5. Temperature dependence of the normalized resistivity for pellets with nominal composition  $\text{Mg}_x^{11}\text{B}_2$  ( $0.8 < x < 1.2$ ).



Figure 5 presents normalized resistance data for eight different  $\text{Mg}_x^{11}\text{B}_2$  pellets. In each case the curve plotted is the average of three or more samples cut from the same pellet. There is far less variation between the different pellets in this case than there was for the case of boron purity (Fig. 2). Figure 6 plots the  $RRR$  values for each of the individual samples (shown as the smaller symbols) as well as the  $RRR$  of the average curve. As can be seen the  $RRR$  values increase slowly from  $\sim 14$  for  $\text{Mg}_{0.8}^{11}\text{B}_2$  to  $\sim 18$  for  $\text{Mg}^{11}\text{B}_2$ . This is followed by a clear increase in  $RRR$  values for excess Mg, with  $\text{Mg}_{1.2}^{11}\text{B}_2$  having an  $RRR$  value of  $\sim 24$ . The important point to note is that even for the most Mg deficient sample the lowest measured  $RRR$  value is significantly greater than 10. At no point in this series we find samples with  $RRR$  values of 3, 6, or 10, even when a clear  $\text{MgB}_4$  second phase is present. For samples ranging from  $\text{Mg}_{0.9}^{11}\text{B}_2$  to  $\text{Mg}_{1.1}^{11}\text{B}_2$  (dotted box in figure 6) the average  $RRR$  values cluster around  $RRR = 18 \pm 3$ . These data indicate that for sintered pellets  $RRR$  values of 18 can be associated with stoichiometric  $\text{Mg}^{11}\text{B}_2$ .

Whereas the effects of excess Mg are relatively minor in these samples (given their low intrinsic resistivities) these effects can be clearly seen. In addition to the increase in the  $RRR$  value there is a change in the form of the temperature dependence of the resistivity. This can be best seen in Fig. 7 in which the

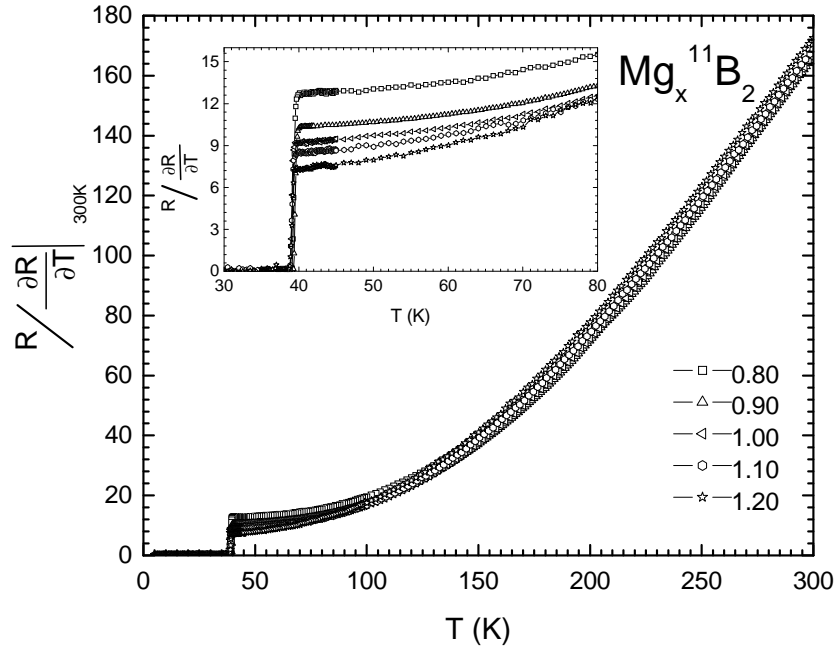


Fig. 6. Residual resistance ratio of  $\text{Mg}_x^{11}\text{B}_2$  ( $0.8 < x < 1.2$ ). The open symbols represent different pieces selected from the same batch. The solid symbols are the average. The dotted box delimits the small variation ( $x \pm 0.1$ ) with respect to the stoichiometric compound.

resistance data have been normalized its room temperature slope. The data for all  $x$  values less than 1.0 are similar and collapse into a single curve. On the other hand the resistance data for the  $x = 1.1$  and  $x = 1.2$  are qualitatively different. They start out with somewhat higher normalized resistance data than the stoichiometric sample and then below 100K cross below the stoichiometric sample (Fig. 7 inset). This is very likely due to the increasing effects of having Mg in parallel (and series) with the  $\text{MgB}_2$  grains. As can be seen in Fig. 7 this effect becomes larger as the amount of excess Mg is increased. This deviation from the  $\text{MgB}_2$  resistance curve may actually serve as a diagnostic for the detection of excess Mg.

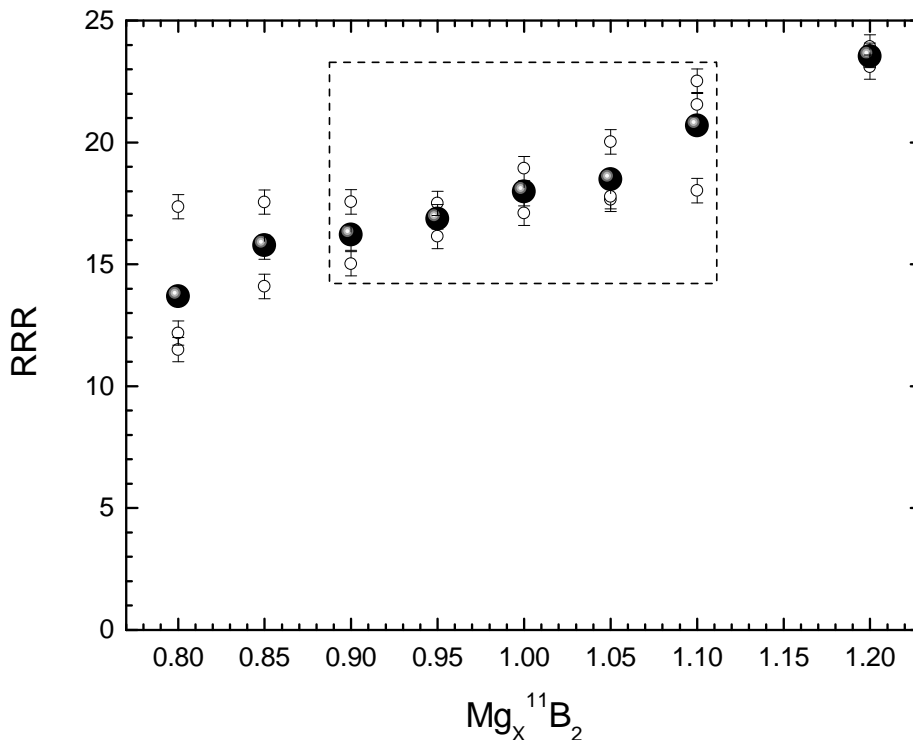


Fig. 7. Resistivity curves normalized by temperature derivative at room temperature, for  $\text{Mg}_x^{11}\text{B}_2$  ( $x = 0.8, 0.9, 1.0, 1.1$  and  $1.2$ ).

## 5 $\text{MgB}_2$ wire segments: Effects of diameter, etching and distilling

$\text{MgB}_2$  can also be synthesized in the form of wire segments [5]. The starting material is boron filament that has a small tungsten-boride core. Upon exposure to Mg vapor the boron filament is transformed into  $\text{MgB}_2$  wire segments, a process that is accompanied by an expansion of the wire diameter. Table 2 presents data on the initial and final diameters of the boron fiber and  $\text{MgB}_2$  wire segments used for this study. There is a clear expansion associated with

the transformation of the boron into  $\text{MgB}_2$ . The average increase in the diameter associated with this reaction is  $\sim 1.4$  times. There is some uncertainty associated with this number due to the fact that once the  $\text{MgB}_2$  is formed the wire segments have a somewhat irregular surface as well as variation of the diameter along the length of a segment. The tungsten boride core does not manifest a noticeable change in diameter during this process. The size of the tungsten boride core of the wire segments is listed on the far side of Table 2. For the rest of this paper the wire segments will be identified by the diameter of the initial boron filament used to create them.

Table 2: Main properties of  $\text{MgB}_2$  wires and resistivity at  $300\text{K}$  and  $RRR$  for as-grown, etched and distilled  $\text{MgB}_2$  filaments with different diameters.(Note: Samples by the diameter of initial boron filaments used.)

Approximate Diameter [ $\pm 10\mu\text{m}$ ]		Approximate Expansion	$\text{WB}_x$ Approximate Diameter [ $\mu\text{m}$ ]
Initial (Boron)	Final ( $\text{MgB}_2$ )		
100	140	1.4	15
140	190	1.5	15
190	290	1.5	15
300	370	1.3	20

Sample Wires		$\rho(300\text{K})[\mu\Omega\text{cm}]$	RRR
AS GROWN	100	13.0	18
	140	10.8	45
	190	8.3	25
	300	14.4	36
ETCHED	100	17.5	39
	140	15.8	30
	190	9.1	45
	300	16.3	28
DISTILLED	300	9.3	35

Given that the wire segments are synthesized in a Mg rich vapor (the nominal stoichiometry is  $\text{Mg}_3\text{B}$ ), there is concern that small amounts of excess Mg vapor condense onto the surface of the  $\text{MgB}_2$  wire segments during the cooling process. This could lead to contributions to the temperature dependent resistivity from metallic Mg. In addition there is the possibility that the tungsten boride core may act as a low resistance resistor in parallel with the

MgB<sub>2</sub>. Measurements of the transport properties of MgB<sub>2</sub> wire segments of varying diameters will allow us to examine, and ultimately discount, both of these concerns.

If there were to be a significant contribution from metallic Mg on the surface of the wire segments, and if it is to be assumed that the metallic Mg has a lower resistivity than the intrinsic resistivity of the MgB<sub>2</sub> (an assumption that is supported experimentally by our earlier data on the Mg<sub>1.2</sub><sup>11</sup>B<sub>2</sub>), then the effect of this excess Mg would scale with the surface area to volume ratio of the sample: i.e. there would be a substantially larger effect seen for the smaller diameter wires than for the larger diameter wires. In a similar manner the potential effect of the tungsten boride core would scale with the square of the ratio of the tungsten boride diameter to the MgB<sub>2</sub> wire diameter. Given that the tungsten boride diameter remains between 15 and 20  $\mu\text{m}$  over the whole series and that the MgB<sub>2</sub> diameter increased from  $\sim 140\mu\text{m}$  to  $\sim 370\mu\text{m}$ , the potential effect that the tungsten boride would have would be largest in the smaller diameter wires and smaller in the larger diameter wires.

The temperature dependencies of the normalized resistivity of MgB<sub>2</sub> wire segments are shown in Fig. 8a. All four diameter wires have similar temperature dependencies, but manifest somewhat different *RRR* values. The inset to Fig. 8a shows the low temperature behavior near  $T_c$ . From this plot it becomes clear that there is no apparent effect of metallic Mg or tungsten boride on the resistivity. The *RRR* values for the 100, 140, 190 and 300  $\mu\text{m}$  wire segments are 18, 45, 41 and 25 respectively. The highest *RRR* value is for 140  $\mu\text{m}$  and the lowest value is for 100  $\mu\text{m}$ . To first order, there appears to be little or no correlation between the wire diameter and the *RRR* values. If any trend is to be extracted it is that *RRR* values are generally higher for the larger diameter wires, a trend that contradicts the assumption that metallic Mg or tungsten boride are affecting the resistivity measurements.

In order to further examine the possible effects of metallic Mg on the transport properties of the wires we etched the as-grown wire segments in a solution of 5% HCl in ethyl alcohol for 5 minutes. This lead to an apparent removal of any Mg coating on the wire surface. The temperature dependence of the normalized resistance of these etched samples are shown in Fig. 8b. In this case the values of *RRR* are increased. If the excess Mg in wires were acting as a parallel resistance in the sense of shorting MgB<sub>2</sub>, we would expect that with its removal we would find smaller *RRR* values, not larger.

In the distillation process, the MgB<sub>2</sub> as-grown wire with 300  $\mu\text{m}$  boron fiber initial diameter, which has *RRR* = 36 was heated to 600°C for 12 hours and submitted to a continuously pumped high vacuum for removal of any excess Mg. This process practically did not alter the value of *RRR*  $\sim 35$ . This is strong evidence that the high values of *RRR* which we obtained for MgB<sub>2</sub>

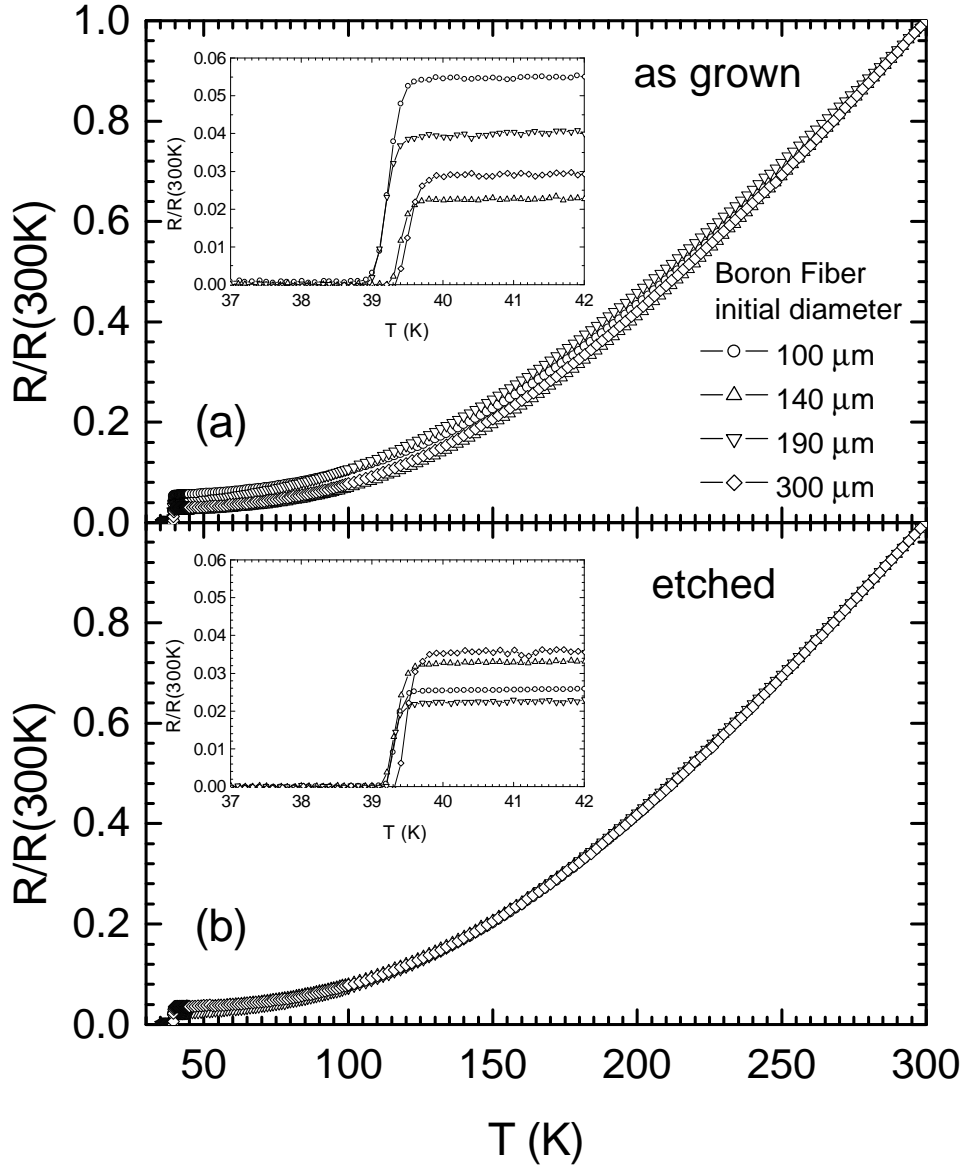


Fig. 8. Resistivity curves of  $MgB_2$  filaments with four boron fiber initial diameters (100, 140, 190 and 300  $\mu m$ ): (a) for as-grown wires and (b) after etched in ethyl alcohol with 5% of HCl.

wires are intrinsic and not an influence of excess Mg.

Table 2 presents our estimates of the room temperature resistivity for each wire sample. The average room temperature resistivity for these nine samples is roughly 13  $\mu\Omega cm$ . It should be noted that the acid etching does increase the

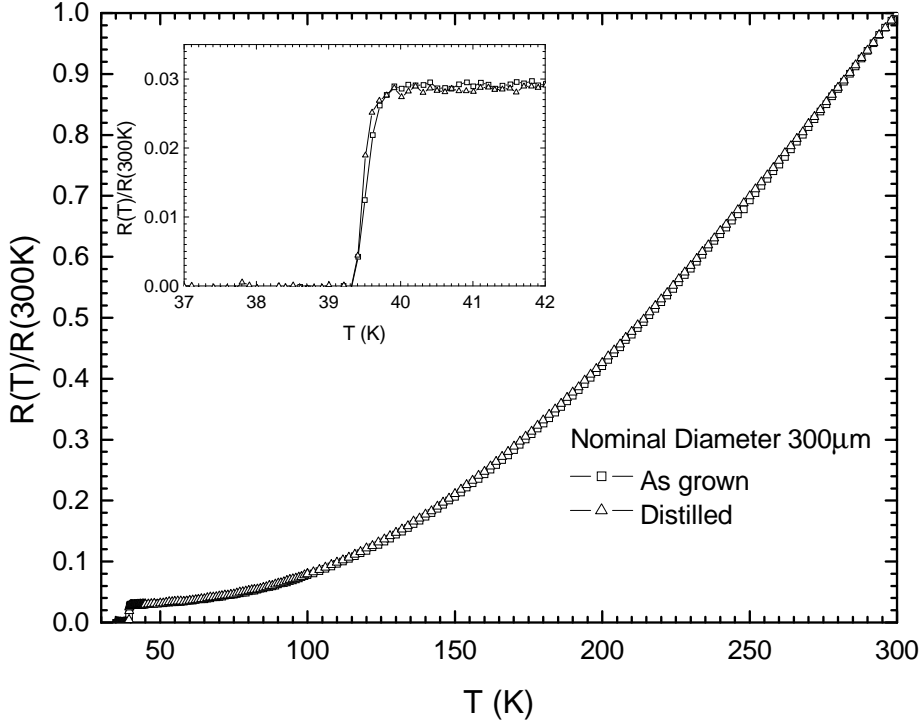


Fig. 9. Resistivity curves before and after distillation process in  $\text{MgB}_2$  wire with  $300\mu\text{m}$  boron fiber initial diameter.

measured resistivity of the wires. We believe that this is due to two effects: i) a reduction of cross sectional area that has not been accounted for and ii) the creation of small cracks in the wire. In both cases the will change the effective geometry of the sample.

A final point about all of the wire samples is worth noting: all of the measured  $RRR$  values are comparable to or better than those found for the stoichiometric  $^{11}\text{B}$  pellet samples. These boron fiber are made using a boron fluoride intermediate step and are reported to be 99.999% pure. This again points out that the purity (and probably the purification process) of the boron may be a critical variable.

## 6 Conclusion

In summary, through the synthesis of various pellets of  $\text{MgB}_2$  with different types of boron we found values of  $RRR$  from 4 to 20, which covers almost all values found in literature. To obtain high values of  $RRR$ , high purity reagents are necessary. With the isotopically pure boron we obtained the high-

est  $RRR \sim 20$  for the stoichiometric compound. We also investigated  $Mg_x^{11}B_2$  samples with  $0.8 < x < 1.2$ . These have shown that from the most Mg deficient samples we observe inclusions of the  $MgB_4$  phase, and no evidence of Mg. For samples with excess Mg we do not observe any  $MgB_4$ . For the range  $Mg_{0.8}^{11}B_2$  up to  $Mg_{1.2}^{11}B_2$  we found average values of  $RRR$  between 14 and 24. For smaller variations in stoichiometry ( $x \pm 0.1$ )  $RRR = 18 \pm 3$ . In addition our study of  $MgB_2$  wires as function of diameter is consistent with pellet results and inconsistent with either Mg or tungsten boride core acting as resistor in parallel with  $MgB_2$  filaments. All of our data are point to conclusion that high  $RRR$  ( $\geq 20$ ) and low  $\rho_0$  ( $\leq 0.4 \mu\Omega cm$ ) are intrinsic materials properties associated with high purity  $MgB_2$ .

## Acknowledgements

Ames Laboratory is operated for the US Department of Energy by Iowa State University under Contract No. W-7405-Eng-82. This work was supported by the Director for Energy Research, Office of Basic Energy Sciences and the National Science Foundation under grant No. DMR-9624778. The authors would like to thank D. K. Finnemore, M. A. Avila and N. Anderson for helpful assistance and many fruitful discussions.

## References

- [1] J. Akimitsu, Symposium on Transition Metal Oxides, Sendai, Janury 10, 2001.
- [2] J. Nagamatsu, N. Nakagawa, T. Muranaka, Y. Zenitani and J. Akimitsu, Nature 410 (2001) 63.
- [3] S. L. Bud'ko, G. Lapertot, C. Petrovic, C. E. Cunningham, N. Anderson and P. C. Canfield, Phys. Rev. Lett. 86 (2001) 1877.
- [4] D. K. Finnemore, J. E. Ostenson, S. L. Bud'ko, G. Lapertot and P. C. Canfield, Phys. Rev. Lett. 86 (2001) 2420.
- [5] P. C. Canfield, D. K. Finnemore, S. L. Bud'ko, J. E. Ostenson, G. Lapertot, C. E. Cunningham and C. Petrovic, Phys. Rev. Lett. 86 (2001 )2423.
- [6] X. H. Chen, Y. S. Wang, Y. Y. Xue, R. L. Meng, Y. Q. Wang and C. W. Chu, Phys. Rev. B 65 (2002) 024502.
- [7] Sang Young Lee, J. L. Lee, Jung Hun Lee, J. S. Ryu, J. Lim, S. H. Moon, H. N. Lee, H. G. Kim and B. Oh, Appl. Phys. Lett. 79 (2001) 3299.
- [8] A. K. Pradhan, Z. X. Shi, M. Tokunaga, T. Tamegai, Y. Takano, K. Togano, H. Kito and H. Ihara, Phys. Rev. B 64 (2001) 212509.

- [9] Kijoon H. P.Kim, Jae-Hyuk Choi, C. U. Jung, P. Chowdhury, Hyun-Sook Lee, Min-Seok Park, Heon-Jung Kim, J. Y. Kim, Zhonglian Du, Eun-Mi Choi, Mun-Seog Kim, W. N. Kang, Sung-Ik Lee, Gun Yong Sung, Jeong Yong Lee, Phys. Rev. B 65 (2002) 100510.
- [10] Y. Y. Xue, R. L. Meng, B. Lorenz, J. K. Meen Y. Y. Sun and C. W. Chu, cond-mat/0105478.
- [11] Filaments with diameters of 100, 140 and 200 $\mu m$  microns were obtained from Textron Systems, 201 Lowell Street, Wilmington MA 01887.
- [12] Filaments with diameter of 300 $\mu m$  were obtained from Goodfellow Corporation, 800 Lancaster Avenue, Berwyn PA 19312-1780.
- [13] C. E. Cunningham, C. Petrovic, G. Lapertot, S. L. Bud'ko, F. Laabs, W. Straszheim, D. K. Finnemore and P. C. Canfield, Physica C 353 (2001) 5.